KnE Engineering

STARTCON19
STARTCON19 - International Doctorate Students Conference + Lab Workshop in Civil Engineering
Volume 2020

Knowledge E
enriching | engaging | empowering

Conference Paper

Stress-strain Relationship in Homogeneous and Two-layered Triaxial Test Specimens

Gabriel Oliveira and Isabel Falorca

C-MADE, Department of Civil and Architectural Engineering, University of Beira Interior, Edifício das Engenharias, Calçada Fonte do Lameiro, 6201-001 Covilhã, Portugal

Abstract

The stress-strain relationship of a homogeneous specimen, obtained from triaxial compression test, allows to determine stiffness parameters for numerical-method based analyses in common geotechnical software. Stiffness parameters are defined as the ratio of stress to strain along an axis. However, when a heterogeneous specimen is tested, the equivalent elastic modulus that represents a simplification of the nonlinear behavior is complex. This paper presents a study intended to contribute to the debate about the degree to which conventional soil mechanics approaches can be applied to layered specimens. Triaxial compression tests were carried out on both homogeneous and two-layered specimens under a low effective confining pressure of 30 kPa. The triaxial apparatus was chosen since the applied stress and specimen boundary conditions are well defined, and the repeatability of the test method is good. The behavior of both specimens was studied in terms of the stress-strain relationship and stiffness. The main differences were crucial to understanding the composite soil-aggregate interaction, which is discussed and compared. The results indicate that the interface between composite soil and aggregate is important to keep the stability of the layer of aggregate over the soft composite soil, and practical methods of achieving that are suggested.

Corresponding Author:
Gabriel Oliveira
gabriel.marchi.oliveira@ubi.pt

Received: 7 January 2020
Accepted: 21 April 2020
Published: 3 May 2020

Publishing services provided by Knowledge E

Selection and Peer-review under the responsibility of the STARTCON19 Conference Committee.

1. Introduction

Triaxial testing of cylindrical soil specimens started in the 1930s [1]. The triaxial compression test is widely used in both the research for understanding and modelling of fundamentals of soil behaviour and in engineering practice for measuring the stress-strain properties of soils. The procedure typically involves subjecting a cylindrical soil specimen to axial compression stress while a constant radial pressure stress is maintained. In the data processing method, it is generally assumed that the soil specimen deforms uniformly during the test and that the intermediate principal stress is equal to the minor principal stress. Thus, the deviator stress, which acts in the axial direction, is calculated from the measured axial load, the axial strain is determined from the measured axial displacement, and the radial strain is simply calculated from the measured

volume change and axial displacement. Test results are usually analysed by the Mohr-Coulomb failure criterion to express the triaxial strength of the soil. Stiffness parameters are defined as the ratio of deviator stress to strain in the direction of the axis of the specimen.

The errors associated with triaxial test should be concerned with all geotechnical engineering purposes as practical field and experimental investigations. The homogeneous specimens do not performer a uniform deformation in the test procedure, it is caused due to many sources of errors associated e.g., sample preparation/sealing, area correction, membrane resistance, frictional ends, seating, filter drain resistance, bedding error, and so forth [2 - 3].

Unlike in the field of rock mechanics which many studies have been developed so far, few studies with heterogeneous samples were performed in a triaxial compression test. This is due to the complex nonlinear behaviour of the variables in natural layered soils to measure the equivalent elastic moduli [4 - 5]. Arthur and Phillips [6] presented important contributions in the area of layered soil. For instance, the effects of anisotropy on the stress-strain curve depends on the proportion of a loose and dense material in the sample, beyond that the loose material dilate much more in a layered soil than in homogeneous samples and the inherent anisotropy do not affect the stress-dilatancy relationship which do not affect the virtual coincidence of stress-strain rate axes.

In nature normally the multi-layered soil stiffness increases with depth [7 – 9]. However, in the unpaved road when there is a weak subgrade, with a California Bearing Ratio equal or less than 3%, an aggregate layer is commonly placed above the soft soil to reinforce the soil-system [10]. To simulate the interface between layered soils in an unpaved road soil system, this research intends to understand the contribution in terms of strength parameters and strain in two-layered specimens with the use of triaxial apparatus.

2. Experimental Method

2.1. Test equipment

The triaxial automated system available at the Soil Mechanics Lab of the University of Beira Interior contains the following primary components to enable the desired stresses to be applied on the specimens, while recording their response. The axial loading device is a velocity controlled 50kN load frame with a speed range of 0.00001mm/min to 5.99999mm/min, which provides an axial movement of the loading platen to shear the

specimen at a constant rate. The axial displacement-measuring device is an external linear variable displacement transducer (LVDT), mounted on a frame which is either attached to the loading ram, have a range of 50mm in which the measurement accuracy was 0.01mm. The axial load-measuring device is an internal submersible electronic load cell which has a measurement range of 16kN and an accuracy of 0.1% of the measurement range.

The triaxial cell to house the specimen and cell fluid is a common passive cell made of aluminium with a perspex wall so the behavior of the specimen may be observed. The specimen top-cap is of rigid aluminium, with a plane surface of contact with the specimen and circular cross-section. The base pedestal also has a plane surface of contact with the specimen and circular cross-section. They have a diameter equal to the initial diameter of the specimen and inlets to provide drainage from both ends of the specimen. The pressure and volume control devices are microprocessor-controlled syringe pumps which have a volumetric capacity of 200cc, a working pressure range of 1MPa and resolutions of 1kPa and 0.001cc. Despite their availability, they were not used in the experimental study due to the stress conditions with selected levels of low confining pressure.

To allow the preparation of the specimens on the pedestal and the measurement of the volume change of the dry specimens throughout tests under low confining pressure, the following additional components were installed in the triaxial cell. The vacuum-control device is a rotary vane vacuum pump capable of producing 2.2 m3/h of free air displacement, which was equipped with a vacuum regulator, pressure range -1200 to 0 mbar and accuracy with response sensitivity less than 2mbar. The volume change measurement device is an Automatic Volume Change Unit with a capacity of 100ml and able to detect volume changes of about 0.05ml, at room temperature under a pressure of 10kPa.

2.2. Materials

Figure 1 shows the grain-size distribution curves of three materials that were used in the specimen preparation. The stone aggregate is a 100% crushed granite supplied by a quarry in the region (Meimoa quarry), which is mapped as a medium- to coarse-grained two-mica granite, with a specific gravity of 2.63. The stone aggregate was sieved to get the required 8-15mm size fraction, classified as GP - poorly graded gravel, according to the Unified Soil Classification System [11]. This aggregate was reused several times, after

being re-sieved on each test. The good hardness of the granite aggregate minimised the amount of particle crushing experienced during shear.

The sand, made of quartz, consists of particles with a relative density of 2.65. The rubber aggregate, resulting from the grinding of used tires, consists of particles with a relative density of 1.16. The mixture of sand and rubber particles was prepared by arrangement in thin layers to avoid segregation of the components and to obtain a homogeneous material. Based on the study carried out by Kim and Santamarina [12], a 55% rubber particle fraction and 33% porosity, defined by the ratio of the rubber volume to the total solids volume, was adopted, resulting in a volume of sand sufficient for fill the voids between the rubber particles. The Figure 2: (a), (b) shows a CBR test equal to 2% carried out in the homogeneous layer of sand-rubber which was used the same particle fraction in the triaxial test.

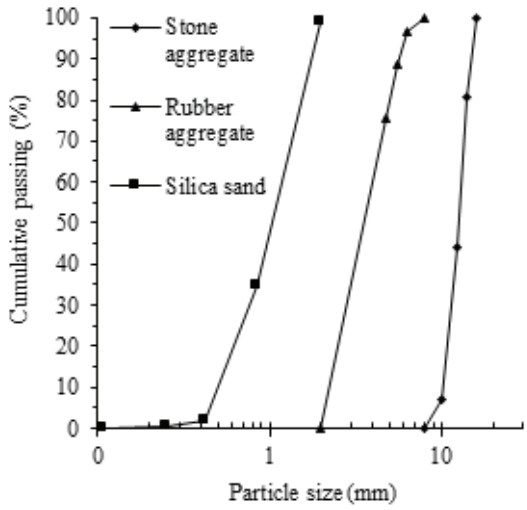

Figure 1: Grain-size distribution curves for test materials.

2.3. Specimen preparation

The preparation specimen concerned in the errors associated with specimen preparation such as leakage, tilting and seating, alignment and frictional end. The rubber membrane was chosen to avoid pinholes and consequently leakage. The end of the aggregate layer was levelled to avoid tilting and seating errors at the top cap. The mould was attached to the pedestal to maintain the alignment of the sample. The polished disc and filter paper were placed on the top and base of the pedestal. The specimen (100 mm diameter and 200 mm height, to minimize dimensional effects) was previously

(a) (b)

Figure 2: CBR test. (a) test apparatus for application of forces (b) test specimen after the test.

jacketed with a rubber membrane (with vacuum) and placed on the triaxial cell pedestal. The procedure consisted of:

• place the mixture of rubber and sand in the lower half of the mold, as described in item 2.2. The unit weight (γc) was 12.03 kN/m^3, estimated from mass weights of the volumetric fractions of the components, corresponding to an initial void ratio (ec) of 0.49;

• place the aggregate in the upper half of the mold in 5 equal layers. The value of the unit weight (γa) was 14.36 kN/m^3, evaluated from the apparent volume and the mass of the aggregate, with an initial void ratio of (ea) 0.80;

• place the top plate and remove the mold by applying a vacuum inside the specimen, sufficient to maintain its geometry;

• place the o-rings in the specimen and confine it with deaired water, set the water confining pressure (10kPa) and vacuum confining pressure (20kPa).

2.4. Test procedure

In this study the apparatus used to perform triaxial compression tests in two-layered cohesionless soil followed ASTM standard [13]. The tests required for the characterisation of the materials related to item 2.2, triaxial compression tests were performed by loading the specimens at a constant rate of deformation. Although pressure control was available in the triaxial cell, it was decided to impose the desired confining tension by applying suction at the base of the specimen utilizing a vacuum, as a backpressure, which made it possible to simplify considerably execution of the test. Each specimen was tested under controlled deformation conditions, imposing the constant axial deformation

rate of 1 mm/min, until an axial extension of 20% was achieved. This extension was evaluated, at each instant, from the relative external displacement and assuming the simplifying hypothesis of uniform distribution of the axial deformation in the specimen.

2.5. Data processing method

During the test the specimen is subjected to stress conditions that attempt to simulate the in-situ stresses. Actual strains within the specimen typically range widely, with the maximum strains at the centre. The average axial strain is defined to be the change in height of the specimen during shearing stage (ΔL) as measured by the LVDT, divided by the length (Lo) at the beginning of the shearing stage, as expressed by Eq. 1. The total volume strain (Eq. 2) is the relation between change in volume of specimen during loading as determined by Automatic Volume Change Unit (ΔV) and initial volume of specimen (V_o).

$$\varepsilon_a = \frac{\Delta L}{L_o} \tag{1}$$

$$\varepsilon_v = \frac{\Delta V}{V_o} \tag{2}$$

The average cross-sectional area of the specimen was corrected throughout the test, see Eq. 3 which is proposed for drained conditions. The deviator stress is calculated through the values obtained by the load cell and the corrected cross-sectional area (Eq. 4). The soil stiffness is estimated from the initial Young's modulus by Eq. 5 where the effective deviator stress (σ'1 – σ'3) was measured in the 0,1% of axial strain (εa).

$$A_c = \frac{A_o(1-\varepsilon_v)}{(1-\varepsilon_a)} \tag{3}$$

$$\sigma'_1 - \sigma'_3 = \frac{P}{A_c} \tag{4}$$

$$E_i = \frac{(\sigma'_1 - \sigma'_3)}{\varepsilon_a} \tag{5}$$

According to Arthur and Phillips [6] the drained angle of shearing resistance (φ) known as the friction angle was used in homogeneous and two-layered specimens as Eq. (6) where R is the stress ratio (σ'_1/σ'_3). Vaid and Sasitharan [14] said that the maximum dilatancy rate is independent of stress path and confining pressure at failure, relative density, and mode of loading (compression or extension). The author proposed for

triaxial compression test ($\sigma_2 = \sigma_3$) a mobilized angle of dilation (ψ) which has a dependent relation with increments of axial and volume strain, see Eq. (7).

$$\varphi = sin^{-1}\left(\frac{R - 1}{R + 1}\right) \tag{6}$$

$$\psi = sin^{-1}\left[\frac{2}{1 + \frac{3}{(d\varepsilon_v/d\varepsilon_a)}}\right] \tag{7}$$

After the course of each test were measured through calipers, diameters of the samples around the half-height of each layer. Further, it allowed to estimate the plastic radial deformations of each sample, for purposes of comparison with the measured volume change.

3. Test Results and Discussion

3.1. Comparison of stress-strain relationship

The stress-strain relationship of homogeneous (HomS) and heterogeneous specimen (HetS) has a scaled difference in the measured axial displacement and hence axial strain. At least two triaxial tests of each sample were performed which reported the repeatability of the experiments was good. The Figure 3: (a) shows the stress-strain behaviour of aggregate and composite HomS layers and HetS. The HetS did not show the real axial strain of the two-layered specimen at a same scaled stress-strain relationship with homogeneous layer, due to the non-uniformity in the deformation. The Figure 3: (b) shows the total volumetric strain variation of HomS and HetS. The total volume strain in HetS did not have any correction. As noted by [6] the volumetric strain of the heterogeneous layer was a combination of the behavior of the two homogeneous layers having a greater tendency for the behavior of the weaker layer.

3.2. Effect of stiffness heterogeneity

As in homogeneous specimens, the deformation is uniform for reasonable strains, although bulging occurs at large strains. The non-uniform stress state in the specimen can be associated with geometric softening [15]. In the course of the test was noted that the geometry of the HetS is altered due to the sudden changing of properties at the interface level, i.e., void ratio, stiffness, grain size, etc. In this way, a sudden change can possibly cause non-uniformity in the measured axial strain. In addition, when an HetS is performed the cross-sectional specimen area is greater than homogeneous

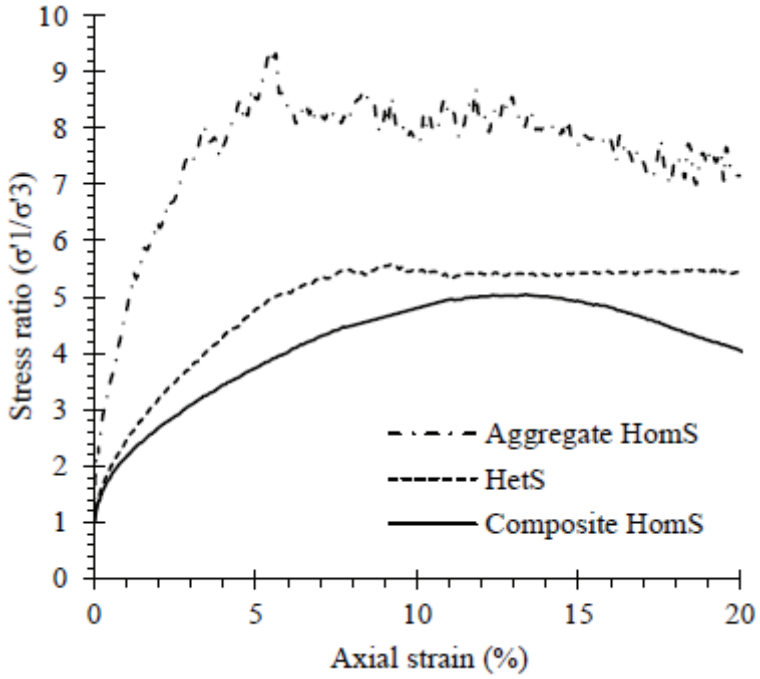

(a)

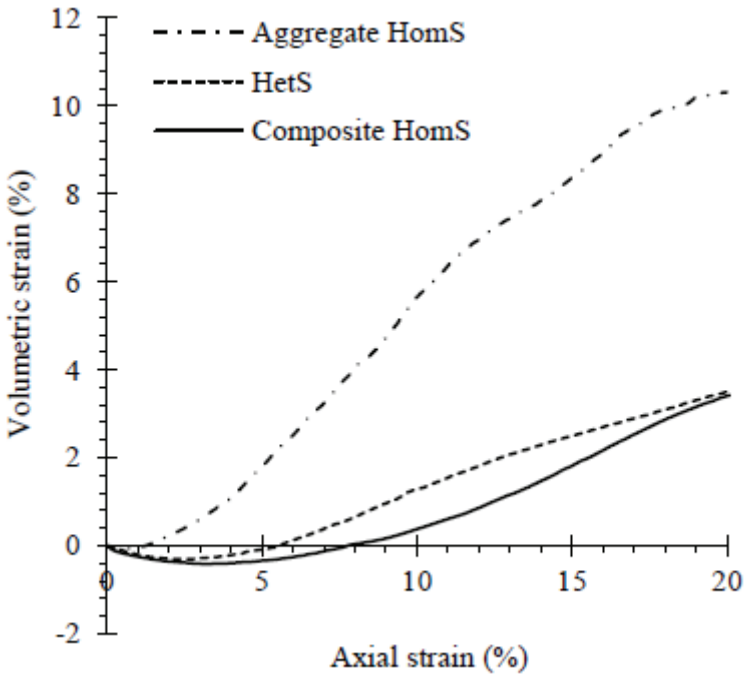

(b)

Figure 3: (a) Stress Ratio versus axial strai (%) at 30 kPa of confining pressure (b) Volume strain (%) versus axial strain (%) at 30 kPa of confining pressure.

samples. A regular cylindrical method [16] calculated the area correction until the peak

strength, after the peak a shear plane was observed thereby the formulation proposed by [17] was used. Figure 4 shows the non-uniform distribution of stress and strain within the specimen. Stiffness parameters are defined as the ratio of stress to strain along an axis. Table 1 shows some of the main parameters. The critical state angle was calculated at 20% of axial strain, in this point the critical state is not yet fully reached but softening and dilation are clearly decreasing. The HetS presented intermediate values of stiffness and dilatancy when compared with aggregate and composite HomS. The HetS showed a stiffness higher than composite HomS, this fact may have been caused by the interlocking of aggregate grains which gave initially a greater stiffness. Figure 5 illustrates the two-layered sample after the test with 20% of axial strain. Different diameters were noted in the half-height of the aggregate layer, at the interface level and in the half-height of the composite layer. Table 2 shows the initial major diameter and the major diameter at 20% of axial strain. At the end of the test an intermediate plastic and volumetric deformation were exhibited at the interface of the HetS when compared with the initial diameter state of both homogeneous layers of the specimen.

TABLE 1: Initial Young's modulus, shear strength and dilatancy of HomS and HetS under triaxial compression.

	E_i(MPa)	φ_{peak} degrees	φ_{cv} [1] degrees	ψ_{peak} degrees
Aggregate HomS	13,62	49,1	41,5	20,9
HetS	5,76	39,7	34,8	15,6
Composite HomS	3,91	36,6	33,3	10,8

[1] cv: critical state

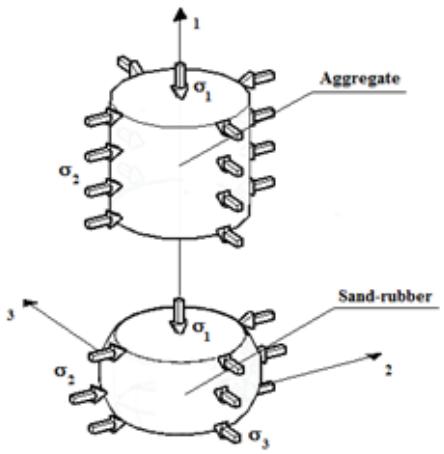

Figure 4: Bulging-type deformation in heterogeneous specimens specimen.

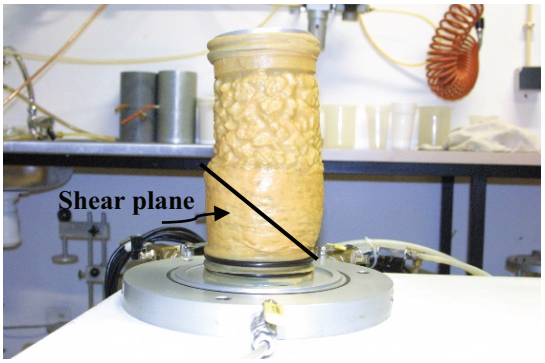

Figure 5: Two-layered specimen at 20% axial strain.

TABLE 2: Major diameter measured with caliper.

	Aggregate HomS	Composite HomS	HetS (agreg./comp.)
Initial Diameter (mm)*	103,4	103,2	103,3/103,4
Diameter at interface level (mm)	-	-	110,3
Diameter at 20% of axial strain (mm)[1]	131,1	119,1	104,2/123,1[1]

[1] major diameter measured in the half-height of HetS

4. Conclusion

The major diameter measured indicated that the interface between aggregate and composite soil there was a sudden changing of stiffness, void ratio and friction angle of the aggregate and rubber–sand mixture. At the interface, level it is important to keep the stability of the layer of aggregate over the soft composite soil through the separation of each layer. The measurements of the diameters at 20% of the axial strain confirmed the variation of volume suffered by the samples at the end of the tests. This investigation with the triaxial compression test of heterogeneous specimens can give insight into the gain of two-layered stiffness with the addition of geosynthetics at the interface. However, the real stress-strain relationship of the heterogeneous specimen is still unknown.

Acknowledge

The lead author would like to gratefully acknowledge the scholarship BID/UBI - Santander Universidades/2018 and the Laboratory of soil mechanics – DECA. This work was also partially financed by Portuguese national funds through FCT – Foundation for

Science and Technology, IP, within the research unit C-MADE, Centre of Materials and Building Technologies, University of Beira Interior, Portugal.

References

[1] A. S. Saada, F. C. Townsend, *STP***740***-EB Laboratory Shear Strength of Soil*, ASTM International, 7 (1981)

[2] J. T. Germaine, C. C. Ladd, *STP***977***-EB Triaxial Testing of Saturated Cohesive Soils*. ASTM International, 421 (1988)

[3] G. Baldi, D. W. Hight, G. E. Thomas, *STP***977***-EB A Re-evaluation of Conventional Triaxial Test Methods*, ASTM International, 219 (1988)

[4] P. J. Guo, F.E. Stolle. *Lower and upper limits of layered-soil strength*, Can. Geotech. J., **46**: 665 (2009)

[5] P. J. Guo, F.E. Stolle. *A physically meaningful homogenization approach to determine equivalent elastic properties of layered soil*, Can. Geotech. J., **55** 303 (2018)

[6] J.R.F. Arthur, A. B. Philips, *Homogeneous and layered sand in triaxial compression*. Géotech., **25** 799 (1975)

[7] J.H. Atkinson, *Anisotropic elastic deformations in laboratory tests on undisturbed London clay*, Géotech. **25**, 357, (1975)

[8] R.E. Gibson, *The analytical method in soil mechanics*, Géotech., **24**, 115, (1974)

[9] G. Gazetas, *Strip foundations on a cross-anisotropic soil layer subjected to dynamic loading*, Géotech., **31**, 161, (1981)

[10] J. P. Giroud, J. Han, *Design method for geogrid-reinforced unpaved roads. II. Calibration and applications*, J. of Geotech. and Geoenv. Eng., **130**, 787 (2004)

[11] ASTM D2487, *Standard Practice for Classification of Soils for Engineering Purposes*, ASTM International (2017)

[12] H.K. Kim, J.C. Santamarina, *Sand–rubber mixtures (large rubber chips)*. Can. Geotech. J., **45**, 1457 (2008)

[13] ASTM D4767, *Standard Test Method for Consolidated Undrained Triaxial Compression Test for Cohesive Soils*, ASTM International (2017)

[14] Y. P. Vaid, S. Sasitharan, *The strength and dilatancy of sand*, Can. Geotech. J., **29**, 522, (1991)

[15] A. Drescher, I. Vardoulakis, *Geometric softening in triaxial tests on granular material*, Géotech., **39**, 291 (1982)

[16] A.W. Bishop, D. J. Henkel, *The measurement of soil properties in the triaxial test* (Arnould, London, 1962)

[17] P. La Rochelle, S. Leroueil, B. Trak, L. Blais-Leroux, R. Tavenas, *STP***977***-EB Observational Approach to Membrane and Area Corrections in Triaxial Tests*, ASTM International (1988)